Annals of Telecommunications

Exploiting Capture and Interference Cancellation for Uplink Random Multiple Access in 5G Millimeter-Wave Networks
--Manuscript Draft--

Manuscript Number:	ANTE-D-18-00173R1
Full Title:	Exploiting Capture and Interference Cancellation for Uplink Random Multiple Access in 5G Millimeter-Wave Networks
Article Type:	Open Topics
Corresponding Author:	Massimiliano Comisso, Ph.D. University of Trieste Trieste, ITALY
Corresponding Author Secondary Information:	
Corresponding Author's Institution:	University of Trieste
Corresponding Author's Secondary Institution:	
First Author:	Fulvio Babich
First Author Secondary Information:	
Order of Authors:	Fulvio Babich
	Massimiliano Comisso, Ph.D.
	Alessandro Cuttin
	Fabio Ricciato
Order of Authors Secondary Information:	

| Abstract: | The forthcoming 5G technology aims to provide massive device connectivity and ultra-high capacity with reduced latency and costs. These features will be enabled by increasing the density of the base stations, using millimeter-wave (mmWave) bands, massive multiple-input multiple-output systems, and non-orthogonal multiple access techniques. The ability to support a large number of terminals in a small area is in fact a great challenge to guarantee massive access. In this context, this paper proposes a new receiver model for the uplink of 5G mmWave cellular networks. The receiver, called Iterative Decoding and Interference Cancellation (IDIC), is based on the Slotted Aloha (SA) protocol and exploits the capture effect alongside the successive IC process to resolve packet collisions. A 5G propagation scenario, modeled according to recent mmWave channel measurements, is used to compare IDIC with the widely adopted Contention Resolution Diversity SA (CRDSA) scheme to show the performance gain of IDIC, when elements of practical relevance, like imperfect cancellation and receive power diversity, are considered. The impact of packet and power diversity is also investigated to derive the preferable uplink random access strategy that maximizes the system throughput according to the offered channel load. |

| Response to Reviewers: | We wish to thank the Editor for managing the review process and all of the referees for their constructive comments, which have prompted us to improve the submitted manuscript. According to these comments, we have properly modified the paper, submitting a revised version that includes all the suggestions provided by the reviewers.. Please consider that a separate file containing the detailed responses has been attached. |

Exploiting Capture and Interference Cancellation for Uplink Random Multiple Access in 5G Millimeter-Wave Networks

**Fulvio Babich · Massimiliano Comisso · Alessandro Cuttin ·
Fabio Ricciato**

Abstract The forthcoming 5G technology aims to provide massive device connectivity and ultra-high capacity with reduced latency and costs. These features will be enabled by increasing the density of the base stations, using millimeter-wave (mmWave) bands, massive multiple-input multiple-output systems, and non-orthogonal multiple access techniques. The ability to support a large number of terminals in a small area is in fact a great challenge to guarantee massive access. In this context, this paper proposes a new receiver model for the uplink of 5G mmWave cellular networks. The receiver, called Iterative Decoding and Interference Cancellation (IDIC), is based on the Slotted Aloha (SA) protocol and exploits the capture effect alongside the successive IC process to resolve packet collisions. A 5G propagation scenario, modeled according to recent mmWave channel measurements, is used to compare IDIC with the widely adopted Contention Resolution Diversity SA (CRDSA) scheme to show the performance gain of IDIC, when elements of practical relevance, like imperfect cancellation and receive power diversity, are considered. The impact of packet and power diversity is also investigated to derive the preferable uplink random access strategy that maximizes the system throughput according to the offered channel load.

F. Babich, M. Comisso, A. Cuttin
Department of Engineering and Architecture,
University of Trieste,
Trieste, Italy
E-mail: {babich@,mcomisso@,alessandro.cuttin@phd.}units.it

This work was performed when F. Ricciato was with
University of Ljubljana,
Faculty of Computer and Information Science,
Ljubljana, Slovenia

1 Introduction

The coming years will see the birth of the next generation 5G network, which aims to overcome the capacity limitations of current 3G/4G cellular systems. Within the wide set of proposals developed to achieve this objective, three enabling technologies, the so called "big three", are expected to be surely adopted: millimeter-wave (mmWave) transceivers, ultra-dense cell planning, and massive multiple-input multiple-output (MIMO) systems [1]. In particular, the interest in mmWaves finds its main reason in the considerable amount of bandwidth still not allocated in the range of frequencies between 30 and 300 GHz. The exploitation of these currently unused resources has necessarily to deal with the considerable attenuations that characterize the mmWave channel, as compared to the conventional microwave (μWave) one [2]. However, the proved usability of such frequencies through high-gain antennas [3–5], and the existence of already standardized medium access control protocols for 60 GHz wireless personal and local area networks [6], have provided encouraging perspectives concerning the transition towards the mmWave portion of the radio spectrum. These advances suggest in fact the possibility of sustaining high data traffic in densely populated cells, finally making massive communications feasible.

In this scenario, a key role will be played by the multiple access protocols, which should be specifically conceived to manage the massive access of many users. The most suitable solution for 5G uplink/downlink operations has been identified in the non-orthogonal multiple access (NOMA) concept [7], which exploits the power diversity that necessarily occurs when a station receives signals from devices located at different distances. This diversity, in fact, simplifies the application

of Successive Interference Cancellation (SIC) to iteratively extract the different waveforms from the received signal. To allow the communication of many users in each 5G cell, so as to give rise to a massive access scenario, the NOMA concept can be combined with the conventional Time Division Multiple Access (TDMA) approach. While, for downlink operations, a NOMA-TDMA scheme can rely on an access coordinated by the 5G Base Station (BS), the uplink operations involving users' authentication or sporadic communications may require the adoption of a contention-based strategy. So far, the random access procedure in cellular networks has been implemented by selecting the widely diffused Slotted Aloha (SA) protocol [8]. An Aloha-like approach is expected also for 5G networks, where the presence of obstacles and the lack of coordination among the mobile devices would make unrealiable the usage of a carrier sensing mechanism [9]. For this reason, extensions of the Aloha scheme have been developed for wireless sensor and local area networks in scenarios highly affected by the hidden terminal problem [10–13]. Even if the Aloha-based strategy is expected to be confirmed for 5G uplink random multiple access, novel functionalities, including NOMA, will be likely added to this scheme for managing a massive access scenario. The recent advances in the implementation of SIC at the PHYsical (PHY) layer of modern receivers has in fact triggered the rethinking of Aloha-like random access methods [14]. The most significant paradigmatic change is that collisions among packets transmitted by different users, previously seen as destructive events to be prevented, are now embraced in the design of a new class of access protocols based on collision-resolution. Among the foundations of this new idea is the Contention Resolution Diversity SA (CRDSA) scheme [15], which combines an iterative SIC process with the transmission of two copies of the same packet in a frame. CRDSA relies in fact on the possibility of cancelling a correctly received packet in a slot to iteratively decode other colliding packets. The relevance of the CRDSA scheme is also proved by its recent introduction in the DVB-RCS2 standard for satellite communications [16]. Further extensions of this approach have been presented by considering variable packet repetition rates [17], packet erasure correcting codes [18,19], packet correcting codes exploiting the interfered segments [20, 21], and multipacket reception [22]. The common aspect of these proposals is that of not specifically accounting for the propagation aspects, since a conventional erasure channel is assumed. Recently, another interesting approach, called Interference Dissolution (ID) has been proposed in [23]. This approach provides significant throughput improvements, but its adoption requires adjustment on both the transceiver and the receiver, thus making less immediate its direct application to legacy systems. These considerations invite to assess the performance of a backward compatible NOMA-TDMA strategy, represented by a SIC-enabled Aloha-based scheme in a practical 5G scenario.

To pursue this objective in a reliable way, it is necessary to examine the system in a realistic mmWave environment, both in terms of channel model and operating conditions. The usually assumed operating conditions for a repetition-based scheme are in fact: *(i) all copies of a successfully decoded packet can be perfectly cancelled*; *(ii) a packet can be successfully decoded only if no other packets are present in the same slot*. Mainly this second assumption is restrictive for many real-world wireless systems, and particularly for 5G, where the reception power variability may enable packet capture. The term "packet capture" in random access networks describes the fact that any practical radio receiver may successfully decode a packet despite the interference received from other (weaker) sources. Even if multiple users send their packets in the same slot of a frame, one of them might be nevertheless captured at the receiver. The capture effect occurs naturally in all radio receivers, regardless of the particular modulation format, whenever the Signal to Interference plus Noise Ratio (SINR) of the strongest packet is sufficiently high. Contention Resolution Diversity Slotted Aloha (CRDSA) was originally designed for satellite systems with perfect power control [16], where neglecting capture justifies the packet diversity strategy. More general studies on CRDSA, including the capture event, have been carried out in [24], by considering an Additive White Gaussian Noise (AWGN) channel. However, mmWave 5G systems are affected by several propagation phenomena, such as small- and mid-scale fading, which may have a strong impact on the final result of a communication. In terrestrial systems (e.g., LoRa [25]), in fact, power diversity is actually present, therefore capture and also residual interference cannot be ignored. It is hence worthwhile to check if the by now established repetition strategy of CRDSA remains preferable when the actual SINR of the packet is taken into account.

To address this issue, the suitability of CRDSA-like solutions for 5G systems with no (or imperfect) power control is in this work critically reconsidered by showing that, in the presence of cancellation residuals and capture, *the preferable strategy is in general hybrid and consists in sending, in each frame, only a single packet copy for high channel loads and two copies for low channel loads*. Besides, we propose a novel receiver algorithm, called Iterative Decoding and Interference Cancellation

(IDIC), which leverages capture alongside nonideal SIC and hence results suitable for implementation in 5G BS receivers for uplink random access. By adopting a realistic 28 GHz channel model including path-loss, shadowing, fading, and noise, we present a theoretical analysis of the capture probability and a simulation-based comparison between IDIC and CRDSA. This comparison shows that the performance gain achievable by IDIC with respect to CRDSA comes without any additional implementation complexity at the receiver side, since capture is a natural occurrence for any receiver.

The paper is organized as follows. Section 2 introduces the system model. Section 3 describes the capture analysis. Section 4 presents the IDIC receiver. Section 5 discusses the numerical results. Finally, Section 6 summarizes the main conclusions.

2 System model

Consider M transmitting users uniformly distributed over a 5G cell identified by a disk $D(O, \rho)$ of center O and radius ρ, and a receiving BS located in O. The users send their packets, which are generated according to a Poisson arrival process of rate λ, with an equal power P_T on a shared channel. The time is subdivided in Random Access Frames (RAFs) of N slots, and each user attempts the transmission of at most one packet in each RAF. All users are assumed frame- and slot-synchronous, and the packet transmission time coincides with the slot duration [15]. Each user can send L copies of its packet in L different slots of each RAF. Successfully decoded packets (i.e., packets for which at least one copy is correctly received) are acknowledged on a separate reliable feedback channel.

2.1 Channel model

Consider the power p_m received by a BS from a generic user m ($m = 1, \ldots, M$) lying at distance d_m. According to the recently characterized mmWave channel model [3], p_m is influenced by the user/BS antenna gains, the path-loss attenuation, and the random variations due to mobility. In particular, p_m can be calculated as [3]:

$$p_m = \frac{P_T G_T G_R \phi_m \psi_m}{1 + \alpha d_m^\beta}, \tag{1}$$

where G_T and G_R are the transmitting and receiving antenna power gains adopted by the user and the BS, respectively; ϕ_m and ψ_m are the realizations of two random variables (r.v.s) Φ_m and Ψ_m modeling the shadowing and the small-scale fading effects, respectively; α and β are the path-loss parameters obtained from the

widely adopted floating intercept model. In (1), d_m is the realization of a r.v. D_m deriving from a uniform distribution inside the disk $D(O, \rho)$ of radius ρ, whose probability density function (pdf) in polar coordinates is given by [26]:

$$f_{D_m, \Omega_m}(d_m, \omega_m) = \frac{d_m}{\pi \rho^2} \mathbb{1}_{[0,\rho] \times [0,2\pi[}(d_m, \omega_m), \tag{2}$$

where $\mathbb{1}_{\mathbf{X}}(y)$ is the indicator function, that is, $\mathbb{1}_{\mathbf{X}}(y) = 1$ if $y \in \mathbf{X}$ and $\mathbb{1}_{\mathbf{X}}(y) = 0$ if $y \notin \mathbf{X}$; Ω_m denotes the r.v. describing the angle between the BS and the user, while ω_m represents its realization. By integrating (2) with respect to ω_m in $[0, 2\pi[$, and then further integrating the result with respect to d_m, one obtains the cumulative distribution function (cdf) of D_m as [26]:

$$F_{D_m}(d_m) = \left(\frac{d_m}{\rho}\right)^2 \mathbb{1}_{[0,\rho]}(d_m) + \mathbb{1}_{[\rho,+\infty[}(d_m). \tag{3}$$

Still concerning (1), the realization p_m of the r.v. P_m is obtained using the recently introduced bounded path-loss model [27], which describes the signal strength attenuation, that is, $1 + \alpha d_m^\beta$, as a monotonically decreasing function of the distance bounded by unity. This model enables to overcome some limitations of the classic unbounded path-loss model when a user may be arbitrarily close to the BS and/or path-loss measures are not available below a certain communication range. In fact, in (1), the experimentally available estimations at 28 GHz of the parameters α and β [3], which represent the floating intercept and the average path-loss exponent, hold just over a certain distance from the BS.

Mid-scale fading, which is one of the most relevant propagation phenomena in mmWave communication, is assumed to follow a log-normal distribution with standard deviation $\tilde{\sigma}$. Thus, the r.v. Φ_m has pdf:

$$f_{\Phi_m}(\phi_m) = \frac{1}{\sqrt{2\pi}\tilde{\sigma}\phi_m} \exp\left(-\frac{\log^2 \phi_m}{2\tilde{\sigma}^2}\right) \mathbb{1}_{\mathbb{R}_{>0}}(\phi_m), \tag{4}$$

where $\mathbb{R}_{>0}$ denotes the set of positive reals. Besides, small-scale fading is assumed Nakagami distributed, thus the pdf of the r.v. Ψ_m is modeled by a gamma density with unit mean and Nakagami parameter $\eta(\geq 1/2)$:

$$f_{\Psi_m}(\psi_m) = \frac{\eta^\eta}{\Gamma(\eta)} \psi_m^{\eta-1} e^{-\eta \psi_m} \mathbb{1}_{\mathbb{R}_{\geq 0}}(\psi_m), \tag{5}$$

where $\mathbb{R}_{\geq 0}$ denotes the set of non-negative reals, and $\Gamma(x)$ represents the Euler gamma function. Observe that all the considered statistics are selected in agreement with the recent measurements carried out in the mmWave domain [3]. In particular, concerning small-scale fading, the experimental channel parameters are derived in [4] assuming a Rice distribution. However, the gamma density may be anyway adopted by recalling the conversion formula involving the Rice factor and the Nakagami parameter [28].

2.2 Capture model

According to the above described mmWave channel, each packet is subject to path-loss, shadowing, and fading, which cause the power diversity among the different packets. Thus, the receiving 5G BS has to handle the decoding of multiple packets subject to random mmWave attenuations and interference, which results from the contention-based access mechanism. To manage this situation according to the CRDSA rules, at the BS side each RAF is iteratively processed up to a maximum number $i_{\max}$ of allowed SIC iterations. For a given RAF, denote by $\mathcal{B}_n$ the set of packets transmitted in the generic slot n ($n = 1, \ldots, N$), and by $\mathcal{A}^i$ the set of packets acknowledged until iteration i ($i = 1, \ldots, i_{\max}$). The Signal of Interest (SoI) in slot n at iteration i is identified by the packet received with the highest power among those remaining in that slot. If the SoI is correctly received, all of its copies are cancelled from the RAF. This cancellation, to be perfectly accomplished, would require the ideal estimation of the received signal amplitude, of the carrier frequency offset, and of the packet timing. Unfortunately, estimation uncertainties occur in practical implementations. This leads to imperfect cancellation and hence residual interference, commonly assumed proportional to the received power by a factor $0 \leq \gamma \leq 1$ [29]. With reference to slot n, identifying as $\mathcal{C}_n^i$ the set of packets cancelled until iteration i, one may determine the set of packets remaining at iteration i ($i = 1, .., i_{\max}$) and containing the SoI as:

$$\mathcal{R}_n^i = \mathcal{B}_n \setminus \left(\mathcal{A}^{i-1} \cup \mathcal{C}_n^{i-1} \right), \tag{6}$$

where, in the case $i = 1$, $\mathcal{A}^0 = \mathcal{C}_n^0 = \emptyset$. Accordingly, the SINR of the corresponding SoI is given by [26, 29]:

$$\mathrm{SINR}_n^i = \max_{m \in \mathcal{R}_n^i} p_m / u_{m,n}^i, \tag{7}$$

in which the undesired signal power is:

$$u_{m,n}^i = \chi_{m,n}^i + r_n^i + w = \sum_{j \in \mathcal{R}_n^i \setminus \{m\}} p_j + \gamma \sum_{j \in \mathcal{C}_n^{i-1}} p_j + w, \tag{8}$$

where $\chi_{m,n}^i$ and r_n^i represent, respectively, the interference due to the remaining (not cancelled) packets and the residual interference due to the cancelled ones (both referred to slot n and iteration i), while w denotes the noise power at the receiving BS. This latter quantity is evaluated as [2]:

$$w = \varrho \cdot B_{\mathrm{W}} \cdot \mathcal{F}, \tag{9}$$

where $\varrho \cong 3.98 \cdot 10^{-21}$ W/Hz is the noise power spectral density, B_{W} is the transmission bandwidth, and $\mathcal{F}$ is the noise figure of the receiver.

Once (7) is evaluated, the SoI is considered successfully decoded (i.e., the corresponding packet is assumed captured) if the condition:

$$\mathrm{SINR}_n^i \geqslant \xi \tag{10}$$

is satisfied for a given SINR threshold ξ. This formulation provides a sufficiently general modeling of the SIC-enabled receiving system, which is able to include both ideal and nonideal operation modes. In fact, by properly selecting the parameters γ and ξ, we can model both the ideal ($\gamma = 0$) and the nonideal ($\gamma > 0$) interference cancellation, as well as the absence ($\xi = \infty$) and the presence ($\xi < \infty$) of capture. The case $\xi = \infty$ indeed corresponds to the requirement of no undesired power for a correct decoding [15], which is the typical condition assumed in the packet erasure channel model. This condition may result conservative in realistic scenarios, since practical receiving systems actually operate with finite ξ values, which, allowing the capture event, enable to investigate its possible benefits in terms of network performance.

3 Capture analysis

To deepen the aspects related to the capture effect, this section presents a theoretical evaluation of the capture probability in a slot n at iteration $i = 1$. To this aim, consider first, with reference to (1), the r.v. $T_m = \zeta/(1 + \alpha D_m^\beta)$, with $\zeta = P_{\mathrm{T}} G_{\mathrm{T}} G_{\mathrm{R}}$. The cdf of this r.v. can be evaluated by using (3) as:

$$F_{T_m}(t_m) = \Pr\{T_m \leq t_m\}$$

$$= 1 - F_{D_m} \left[\frac{1}{\alpha} \left(\frac{\zeta}{t_m} - 1 \right)^{\frac{1}{\beta}} \right]$$

$$= \left\{ 1 - \frac{1}{\rho^2} \left[\frac{1}{\alpha} \left(\frac{\zeta}{t_m} - 1 \right)^{\frac{2}{\beta}} \right] \right\} \mathbb{1}_{\left[\frac{\zeta}{1+\alpha\rho^\beta}, \zeta \right]}(t_m)$$

$$+ \mathbb{1}_{]\zeta, +\infty[}(t_m). \tag{11}$$

To subsequently estimate the impact of small-scale fading, one has to evaluate the cdf of $Q_m = T_m \Psi_m$ by adopting the product distribution as [5]:

$$F_{Q_m}(q_m) = \int_0^{+\infty} F_{T_m} \left(\frac{q_m}{\psi_m} \right) f_{\Psi_m}(\psi_m) \mathrm{d}\psi_m. \tag{12}$$

In general, the use of (5) and (11) in (12) does not provide closed-form expressions. However, the measurements carried out in [4] have derived a specific value for the Rice factor, which, using [28, eq.(2.49)], enable to identify the corresponding value $\eta = 3$ for the Nakagami parameter. Exploiting this experimental result, one can substitute (11) and (5) for $\eta = 3$ in (12), and

then solve the integral, thus obtaining, after some manipulations, the cdf of Q_m as:

$$F_{Q_m}(q_m) = \frac{1}{2}\left\{2 - \Gamma\left[3, q_m\left(\frac{3}{\zeta} + \nu\right)\right] - \exp\left(-\frac{3q_m}{\zeta}\right)\right.$$

$$(\nu q_m)^{-\frac{2}{\beta}} \sum_{k=0}^{2}\binom{2}{k}\left(\frac{\zeta}{3q_m}\right)^{k-2}\left[\Gamma\left(\frac{2}{\beta}+k+1\right)\right.$$

$$\left.\left.-\Gamma\left(\frac{2}{\beta}+k+1, \nu q_m\right)\right]\right\}\mathbb{1}_{]0,+\infty[}(q_m), \qquad (13)$$

where $\nu = 3\alpha\rho^{\beta}/\zeta$ and $\Gamma(\cdot, x)$ denotes the upper incomplete gamma function. Now, to derive the cdf of $P_m = Q_m\Phi_m$, which additionally accounts for shadowing, one should again apply the product distribution using (4) and (13) as:

$$F_{P_m}(p_m) = \int_0^{+\infty} F_{Q_m}\left(\frac{P_m}{\phi_m}\right) f_{\Phi_m}(\phi_m)\mathrm{d}\phi_m. \qquad (14)$$

Also in this case the direct approach does not provide analytical expressions, thus it becomes necessary to introduce suitable approximations. A useful technique for the products involving normal or log-normal r.v.s has been proposed in [30]. This technique relies on an improved Gaussian approximation, which has the advantage of leading to computationally efficient expressions. Accordingly, the cdf of P_m can be estimated by [30]:

$$F_{P_m}(p_m) \cong \frac{1}{3}\sum_{j=-1}^{1} 2^{1-2|j|} F_{Q_m}\left(\frac{p_m}{\epsilon^j}\right), \qquad (15)$$

where $\epsilon = \exp(\sqrt{3}\tilde{\sigma})$. In a generic slot n at iteration $i = 1$, the residuals due to past SIC are not even present, that is, $r_n^1 = 0$. Hence, the r.v. representing the undesired power $U_{m,n}^1$ at $i = 1$ is given by the sum between the noise and the power received from the $M_n(\leq M - 1)$ interferers initially present in the n-th slot. Adopting the strongest interferer approximation [26], one can therefore approximate the undesired power for the m-th user in slot n at iteration $i = 1$ as:

$$U_{m,n}^1 \cong \max(P_1, ..., P_{M_n}) + w, \qquad (16)$$

where the r.v.s $P_{m'}$ $(m' = 1, ..., M_n)$ have the same cdf of P_m, i.e., the powers received from the different sources are independent and, operating on a channel with the same statistics, are identically distributed. By consequence, applying the rules for the maximum and the translation of r.v.s one obtains the cdf of $U_{m,n}^1$ as:

$$F_{U_{m,n}^1}(u_{m,n}^1) \cong F_{P_m}^{M_n}(u_{m,n}^1 - w). \qquad (17)$$

Once the statistics of the desired and of the undesired powers are available, one can evaluate the capture probability. Recalling condition (10), this latter quantity is

Table 1 Adopted PHY layer parameters [2–4].

Parameter	Value	
M: Number of users	400	
ρ: Disk radius	50	m
P_{T}: Transmission power	20	dBm
N: Number of slots	100	
G_{T}: Antenna transmitting gain	30	dB
G_{R}: Antenna receiving gain	3	dB
α: Path-loss floating intercept	69.8 dB (LOS) 82.7 dB (NLOS)	
β: Average path-loss exponent	2.0 dB (LOS) 2.7 dB (NLOS)	
$\tilde{\sigma}$: Shadowing standard deviation	5.8 dB (LOS) 7.7 dB (NLOS)	
η: Nakagami parameter	3	
B_{W}: Transmission bandwidth	1	GHz
$\mathcal{F}$: Noise figure	10	dB

given by the complementary cdf (ccdf) of the SINR calculated at ξ. Hence, using the ratio distribution, the capture probability for the m-th user in slot n at iteration $i = 1$ can be estimated as:

$$C(\xi, M_n) = \Pr\{\mathrm{SINR}_n^1 \geq \xi\}$$

$$= \int_0^{+\infty} F_{U_{m,n}^1}\left(\frac{p_m}{\xi}\right) f_{P_m}(p_m)\mathrm{d}p_m, \qquad (18)$$

where:

$$f_{P_m}(p_m) = \frac{\mathrm{d}F_{P_m}}{\mathrm{d}p_m}$$

$$\cong \frac{1}{3}\sum_{j=-1}^{1}\frac{2^{1-2|j|}}{\epsilon^j}\left.\frac{\mathrm{d}F_{Q_m}}{\mathrm{d}q_m}\right|_{q_m = \frac{p_m}{\epsilon^j}}, \qquad (19)$$

is the pdf of P_m. By using (15) and (17) in (18), one finally obtains:

$$C(\xi, M_n) \cong \frac{1}{9}\sum_{j,j'=-1}^{1}\frac{2^{2(1-|j|-|j'|)}}{\epsilon^{j'}}\int_0^{+\infty}\left\{\left.\frac{\mathrm{d}F_{Q_m}}{\mathrm{d}q_m}\right|_{q_m = \frac{p_m}{\epsilon^{j'}}}\right.$$

$$\left.F_{Q_m}^{M_n}\left[\frac{1}{\epsilon^j}\left(\frac{p_m}{\xi} - w\right)\right]\right\}\mathrm{d}p_m, \qquad (20)$$

which, employing (13), provides the capture probability at the first iteration by a unique integral operation.

3.1 Validation

This subsection presents the validation of the above developed theoretical model, which is implemented in Matlab using the parameters in Table 1. The values of these parameters are inferred from the recent measurements obtained for the 28 GHz channel in both Line Of Sight (LOS) and Non-LOS (NLOS) conditions
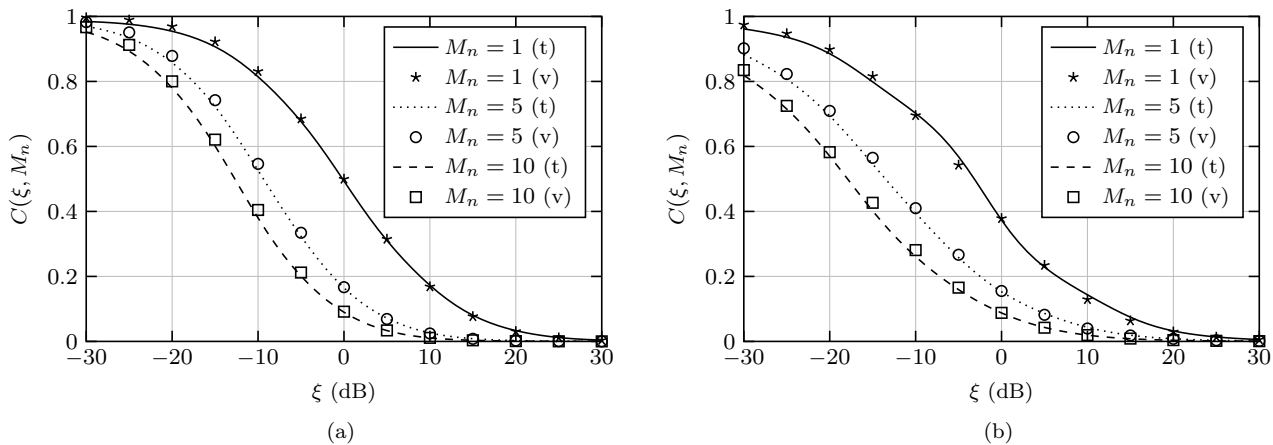
Fig. 1 Capture probability in a generic slot at the first iteration as a function of the SINR threshold for different values of the number of interferers: (a) LOS, (b) NLOS (t: theory, v: Monte Carlo validation).

[3, 4]. As specified during the development of the capture analysis, the value $\eta = 3$ for the Nakagami parameter has been inferred from that of the Rice parameter estimated in [4], by using the conversion formula in [28, Sec. 2.1.2]. Besides, the directional transmitting antenna power gain $G_{\mathrm{T}} = 10 \log_{10}(K^2)$ (in dB) derives from the usage of an array with $K = 32$ radiating elements [3]. The reception is assumed omni-directional with a receiving power gain of 3 dB. The results are shown in Fig. 1, which reports the capture probability in a generic slot at the first iteration as a function of the SINR threshold for different values of M_n in LOS (Fig. 1(a)) and NLOS (Fig. 1(b)) scenarios. The curves obtained from the analysis are represented by lines, while those derived from independent Monte Carlo simulations are represented by markers. The significant matching between theory and simulations proves the accuracy of the developed analysis, further revealing that, when the ξ value and the number of interferers are sufficiently high, the capture probability becomes almost insensitive to the link state (i.e., LOS or NLOS). Otherwise, the LOS scenario provides a higher capture probability with respect to the NLOS one. One may also notice that the $C(\xi, M_n)$ reduction when the number of interferers increases from $M_n = 1$ to $M_n = 5$ is higher than that observed when M_n increases from $M_n = 5$ to $M_n = 10$, since, in the set of the M_n interfering sources, the main impact on the capture probability is given by the subset of the strongest ones.

4 Iterative Decoding and Interference Cancellation (IDIC) receiver

According to the system model introduced in Section 2, the here presented IDIC receiver is explicitly designed

to work in realistic operational conditions, characterized by the possibility of capturing an interfered packet and the presence of imperfect cancellation. The IDIC implementation for a 5G receiving BS is summarized in Algorithm 1. The input quantities are the parameters ξ (SINR threshold), γ (fraction of residual interference), $i_{\max}$ (maximum number of SIC iterations), and $\mathcal{B}_n$ for $n = 1, \ldots, N$ (set of packets present in each of the N slots of the RAF). The algorithm develops as follows.

At the generic iteration i, two main operations are performed by IDIC in each RAF: the checking of the capture events, and the SIC of the possible copies of each captured packet. The first operation is carried out for each slot by using (6)-(10) to verify whether the SoI in the presence of uncancelled and residual interference can be decoded, and hence the corresponding packet $\hat{m}$ can be added to the set $\mathcal{D}$ of the successfully received packets at that iteration. This set is then used to update the set $\mathcal{A}^i$ of the packets decoded until iteration i, and to perform the SIC operation, involving the update of a third set $\mathcal{C}_n^i$, containing the packets cancelled in slot n until i. The RAF processing is then iterated until no more packets can be decoded or the maximum number of allowed iterations is reached. Observe that the order of the two operations involved in the IDIC receiver, that is, capture and SIC, is not due to a choice in the design, but to the natural evolution of the receiving process. In fact, when the capture event occurs, it is spontaneous, and cannot be forced to happen before other implemented operations. In this sense, the IDIC receiver takes advantage of a beneficial, yet unavoidable, random occurrence. Moreover, IDIC is sufficiently general to operate also when multiple packet replicas are generated, that is, when packet diversity is implemented. Thus, in the following, IDIC-L will be used to denote an IDIC receiver operating when a 5G user

Algorithm 1 IDIC receiver

Require: ξ; γ; $i_{\max}$; $\mathcal{B}_n$, $n = 1, \ldots, N$

1: initialize: $i \leftarrow 1$; $\mathcal{A}^0 \leftarrow \emptyset$; $\mathcal{C}_n^0 \leftarrow \emptyset$, $n = 1, \ldots, N$
2: **repeat**
3:     initialize: $\mathcal{D} \leftarrow \emptyset$
4:     <u>Capture</u>
5:     **for** $n = 1, \ldots, N$ **do**
6:         evaluate: $\mathcal{R}_n^i$ by (6)
7:         **if** $\sum_{m \in R_n^i} p_m > 0$ **then**
8:             evaluate: SINR_n^i by (7) and (8)
9:             **if** $\text{SINR}_n^i \geqslant \xi$ **then**
10:                 evaluate: $\hat{m} \leftarrow \underset{m \in \mathcal{R}_n^i}{\arg\max} \dfrac{p_m}{u_{m,n}^i}$
11:                 update: $\mathcal{D} \leftarrow \mathcal{D} \cup \{\hat{m}\}$
12:             **end if**
13:         **end if**
14:     **end for**
15:     update: $\mathcal{A}^i \leftarrow \mathcal{A}^{i-1} \cup \mathcal{D}$
16:     <u>SIC</u>
17:     **for** $n = 1, \ldots, N$ **do**
18:         update: $\mathcal{C}_n^i \leftarrow \mathcal{C}_n^{i-1}$
19:         **foreach** $\hat{m} \in \mathcal{D}$ **do**
20:             **if** $\hat{m} \in \mathcal{R}_n^i$ **then**
21:                 update: $\mathcal{C}_n^i \leftarrow \mathcal{C}_n^i \cup \{\hat{m}\}$
22:             **end if**
23:         **end foreach**
24:     **end for**
25:     $i \leftarrow i + 1$
26: **until** $\mathcal{D} \neq \emptyset \wedge i \leqslant i_{\max}$
27: **return** $\mathcal{A}^i$

can send L packet copies in each RAF to the receiving BS. Thanks to this capability, IDIC can be compared with the widely adopted CRDSA scheme, which is characterized by the usage of $L = 2$ packet replicas in the RAF [15]. To this aim, we consider for IDIC-L the cases $L = 1$ and $L = 2$, and we select $\gamma = 0.1$, and, initially, $\xi = 3$ dB as SINR threshold. According to [29], the value $\gamma = 0.1$ is identified as a good compromise between an overly optimistic situation ($\gamma = 0$) and a scenario where the presence of the residual interference makes the SIC process almost ineffective ($\gamma = 0.5$). With reference to the two considered solutions, IDIC-1 represents a SIC-enabled framed SA system with capture. Observe that, when CRDSA or IDIC-2 are employed, both packet copies are cancelled if at least one of them is successfully decoded. The difference lies in the rule for a successful reception, which, in CRDSA, occurs if at least one of the two copies of the packet is received in a slot containing a unique packet. In IDIC-2, instead, the same event occurs if at least one of the two copies of the packet is received in a slot where its SINR is higher or equal to the threshold ξ. Besides, IDIC-2 is designed to realistically operate in the presence of nonideal SIC.

Table 2 IDIC and CRDSA settings.

| Scheme	γ	ξ (dB)	L
IDIC-1	0.1	3	1
IDIC-2	0.1	3	2
CRDSA-ideal SIC	0	∞	2
CRDSA-nonideal SIC	0.1	∞	2

Concerning this latter aspect, we consider the CRDSA performance with perfect and imperfect cancellation to have a touchstone in both ideal and practical scenarios. The settings for the four compared solutions are summarized in Table 2.

It is worth to observe that the IDIC scheme can be also seen as a kind of message passing algorithm similar to that proposed in [31], but focused on intra-frame cancellation. In particular, in [31], the receiver identifies the slot positions where the same packet was transmitted in all the past RAFs, and therefore cancel it from the signals received in further RAFs. Consequently, when referred to inter-frame cancellation, [31] is an extension of IDIC, but for the sole case $L = 1$, (i.e., for IDIC-1), while, when referred to intra-frame cancellation, IDIC represents an extension of [31] for what concerns its application to the mmWave channel and the possibility of transmitting L copies of a packet in a RAF (in [31], the transmission of just one copy per RAF is assumed).

The IDIC receiver and the CRDSA scheme are implemented in Matlab. Their performance is obtained by Monte Carlo simulations using the parameters in Tables 1 and 3. In particular, with reference to Table 1, the conservative choice of assuming an omnidirectional reception with a receiving power gain of 3 dB is made. Even if omnidirectional antennas operating in the mmWave band with higher gains are commercially available [32], the choice of assuming just a 3 dB receiving gain is done with the purpose to check the IDIC capabilities in ordinary conditions, namely, without using high-end components. Furthermore, the directional transmission-omnidirectional reception context is consistent with the modeled 5G uplink random access scenario, in which M contending users steer the main lobe of their radiation pattern towards the 5G BS that must be capable of simultaneously receiving all the transmitted packets, subsequently beginning the RAF process-

Table 3 Adopted access parameters

Parameter	Value
M: Number of users	400
N: Number of slots	100
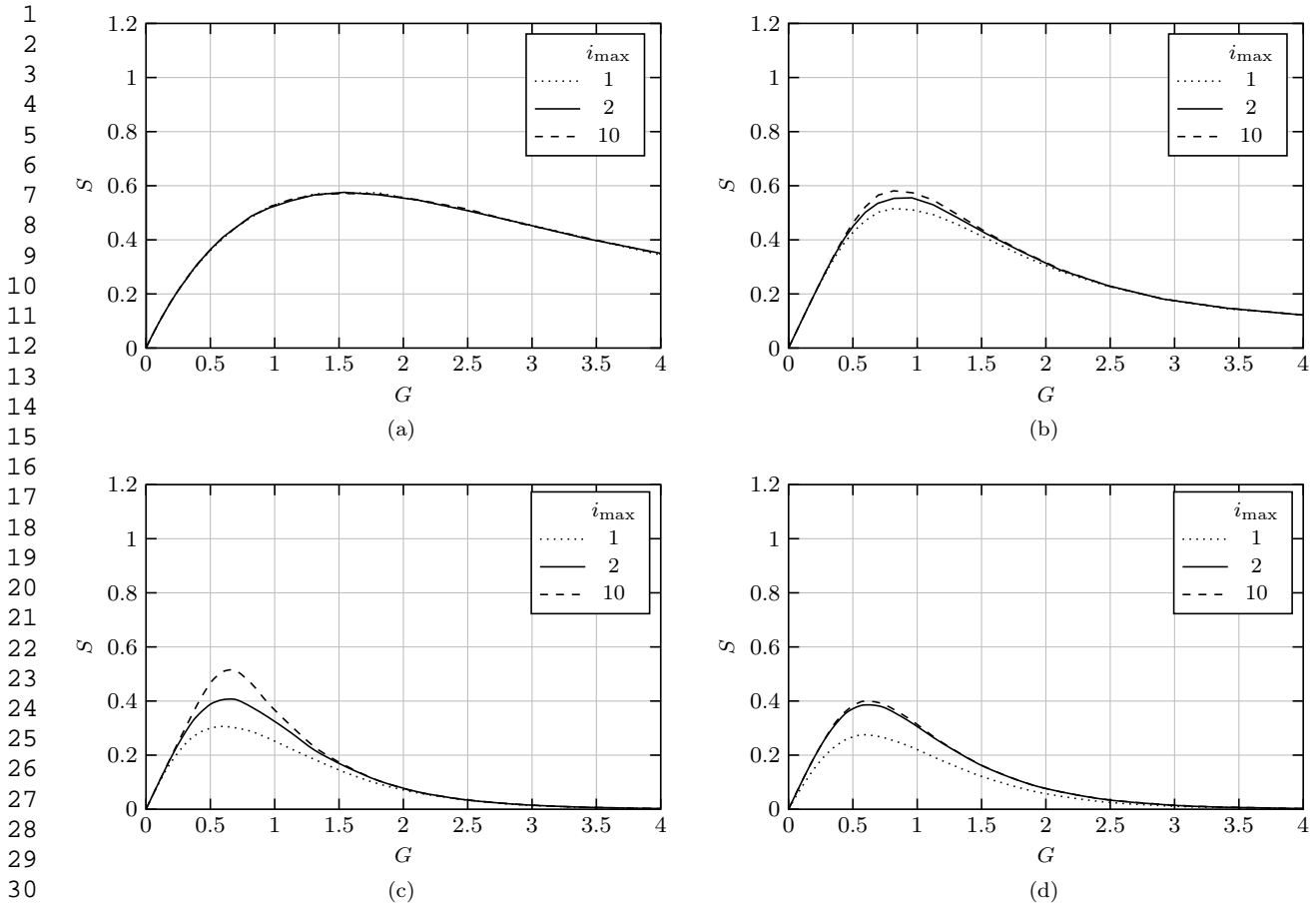
Fig. 2 Throughput vs. input load for different values of the maximum number of iterations in the presence of sole path-loss attenuation considering LOS conditions: (a) IDIC-1, (b) IDIC-2, (c) CRDSA-ideal SIC, (d) CRDSA-nonideal SIC.

ing to establish which packets have been captured and hence which replicas can be cancelled.

5 Numerical Results

This section presents the results obtained from the numerical implementation of the IDIC-L receiver. The adopted performance figures are the network throughput S and the average Packet Loss Rate (PLR). The throughput is evaluated as a function of the input load $G = M\lambda$ [15]. Since both S and λ are measured in packets/slot, S represents the average number of successfully received packets per slot, while G identifies the average number of packets generated per slot. The simulations are run by randomly generating $V = 100$ user topologies within the disk $\mathrm{D}(O, \rho)$, and then considering $H = 1000$ RAFs for each topology. The throughput is estimated by averaging the results over the topologies and the RAFs. Thus, S is estimated as:

$$S = \frac{1}{V} \sum_{v=1}^{V} \left[\frac{1}{H} \sum_{h=1}^{H} \frac{\mathcal{A}_{h,v}^{i_{\max}}(G)}{N} \right], \quad (21)$$

where $\mathcal{A}_{h,v}^{i_{\max}}(G)$ is the number of packets successfully decoded in the h-th RAF and v-th topology after $i_{\max}$ iterations for an input load G, while N is the number of time slots contained in a single RAF.

The PLR, which is still evaluated as a function of G, represents instead the fraction of successfully received packets with respect to the transmitted ones. This quantity, which accounts for the losses due to both the propagation environment and the interference, is hence calculated from S in (21) as:

$$PLR = 1 - \frac{S}{G}. \quad (22)$$

5.1 Impact of packet diversity

The first set of results shows the throughput as a function of the input load for IDIC-1 (Fig. 2(a)), IDIC-2 (Fig. 2(b)), CRDSA with ideal (Fig. 2(c)) and nonideal (Fig. 2(d)) SIC. Each subfigure reports the curves for three values of the maximum number of iterations $i_{\max} \in \{1, 2, 10\}$. These values have been chosen to highlight the characteristics of the IDIC receiver in the dif-
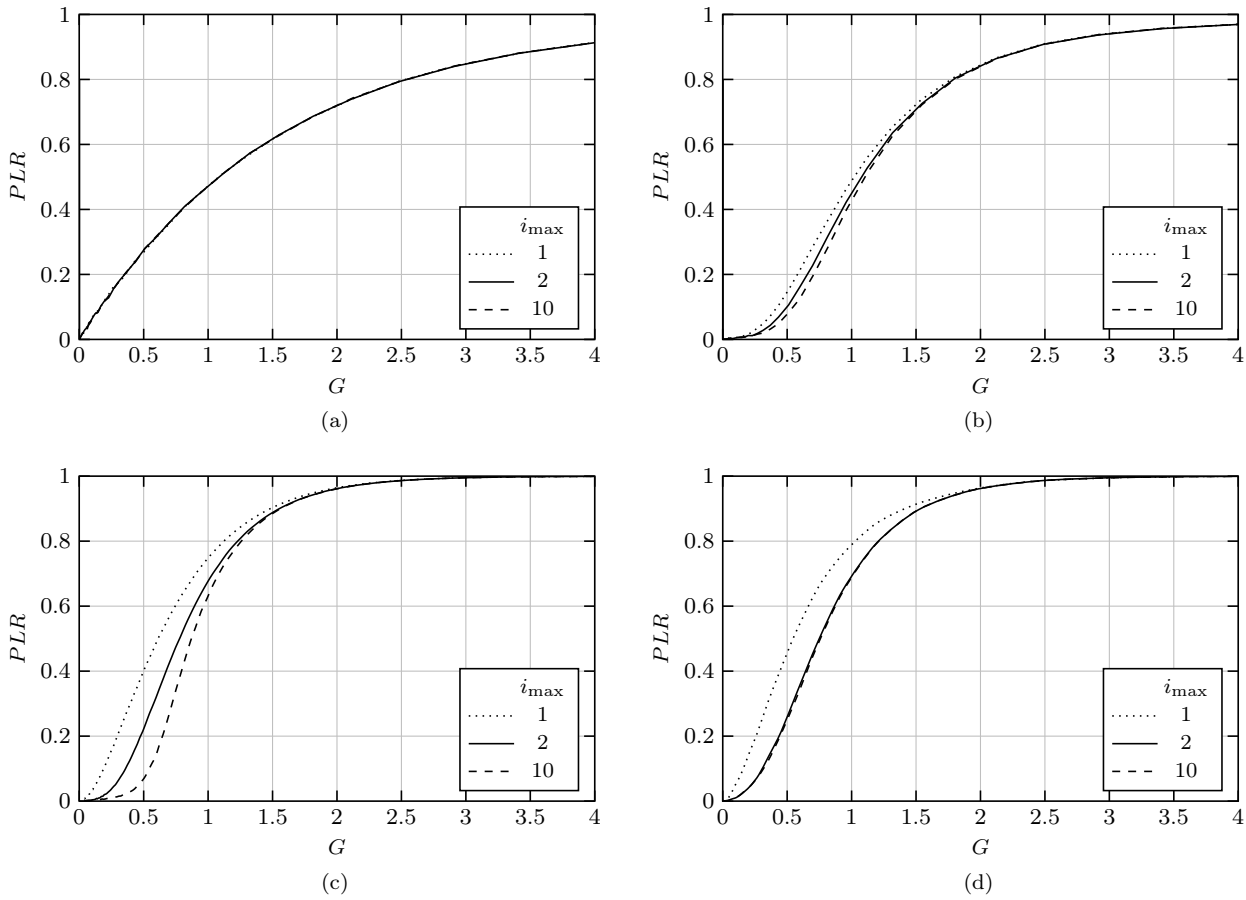
Fig. 3 PLR vs. input load for different values of the maximum number of iterations in the presence of sole path-loss attenuation considering LOS conditions: (a) IDIC-1, (b) IDIC-2, (c) CRDSA-ideal SIC, (d) CRDSA-nonideal SIC.

ferent scenarios, while considering $i_{max} = 10$ as a limit to maintain an acceptable trade-off between the achievable throughput gain and the computational burden at the receiver. The figure is obtained considering LOS conditions and just path-loss attenuation.

A comparison between Figs. 2(a,b) and Figs. 2(c,d) shows the performance improvement provided by the IDIC receiver with respect to the CRDSA-based solutions. This improvement involves not only S, but, also and significantly, the input load corresponding to the maximum throughput, which is approximately equal to 1.5 for IDIC-1 and to 0.9 for IDIC-2. Furthermore, unlike CRDSA, the IDIC approach ensures that the network is still operational even under heavy load conditions. In fact, while the throughput of CRDSA quickly degrades after its maximum, that of IDIC remains acceptable. According to [15], a direct view of Figs. 2(c,d) confirms that an imperfect cancellation influences the CRDSA throughput, but does not have a significant impact on the input load corresponding to the maximum, which remains substantially unmodified in the two cases.

A focused comparison between IDIC-1 and IDIC-2, which adopt the same receiver operation but differ in the number of transmitted copies, reveals two interesting aspects. Firstly, IDIC-1 and IDIC-2 achieve a really similar maximum throughput, but at different G values. This indicates that, when the receiver exploits the capture effect, notwithstanding the non-zero cancellation residual, sending two packet copies in each RAF (as in CRDSA) is useful for low channel loads. Conversely, sending a single packet copy in each RAF becomes advantageous for higher channel loads. Thus, packet diversity may be not always preferable, and the optimal strategy is hybrid. The second aspect that may be noticed is that, in all cases characterized by a non-ideal cancellation, thus also including CRDSA with imperfect SIC, few iterations ($i_{max} = 1, 2$), are sufficient to achieve a throughput very close to the maximum one ($i_{max} = 10$). This aspect, which provides significant benefits in terms of decoding delay, is taken to the extremes by IDIC-1, in which the curves corresponding to the three maximum iterations are almost superimposed. A further observation may be formulated by noticing that
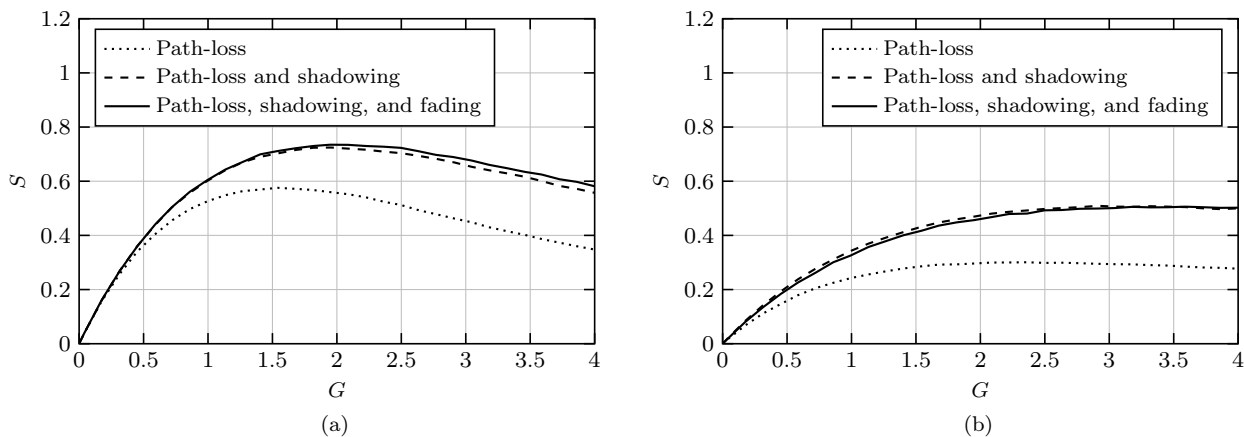
Fig. 4 Throughput vs. input load for IDIC-1 with $i_{\max} = 10$ in different channel conditions: (a) LOS, (b) NLOS.

IDIC-2 outperforms CRDSA with ideal SIC, which reveals that the benefit of exploiting capture dominates over the penalty of having a cancellation residual.

This latter observation is confirmed by Fig. 2, which reports the PLR as a function of the input load for IDIC-1 (Fig. 3(a)), IDIC-2 (Fig. 3(b)), CRDSA with ideal (Fig. 3(c)) and nonideal (Fig. 3(d)) SIC. In particular, one may notice that, when IDIC-L is adopted, the PLR remains lower than one even for high G values.

To better characterize the relationship between IDIC-1 and IDIC-2, let denote as $S_{\text{IDIC}-L}(G)$ the function that maps the input load G to the throughput of IDIC-L. Using this notation, one can derive the following lower bound for the throughput of IDIC-2 with respect to that of IDIC-1:

$$S_{\text{IDIC}-2}(G) > S_{\text{IDIC}-1}(2G) - \frac{S_{\text{IDIC}-1}^2(2G)}{4G}. \qquad (23)$$

The proof of (23) can be obtained through combinatorial considerations. In fact, IDIC-2 with input load G generates an overall load $2G$ (2 replicas per packet) on the physical channel, resulting in a burst decoding probability:

$$p_{bst} = \frac{S_{\text{IDIC}-1}(2G)}{2G}. \qquad (24)$$

Neglecting the fact that decoding a single burst triggers the cancellation of the other (non-decoded) one, one can infer a lower bound on the actual throughput performance. Since the decoding of a single burst of the pair is sufficient to decode the input packet, the packet decoding probability can be related to the burst decoding probability by:

$$p_{pkt} > 2p_{bst} - p_{bst}^2. \qquad (25)$$

Recalling that $p_{pkt} = S_{\text{IDIC}-2}(G)/G$, one finally obtains (23).

We remark that the IDIC improvements are achieved without introducing any additional complexity at the receiver side with respect to CRDSA, since the capture effect is naturally present in any receiver, while the cancellation procedure is already required by CRDSA. A further specific advantage of IDIC is that of providing similar maximum throughput values regardless of the adoption of packet diversity. Hence, if a system designer would select IDIC-1 for a 5G BS receiver, it may benefit of a significant advantage over repetition-based schemes, consisting in the easier adoption of IDIC-1 in legacy framed SA systems, where the user's transmitter is programmed to send one packet copy per RAF. In fact, the introduction of CRDSA requires changing or reprogramming all sources to enable the transmission of packet copies, while IDIC-1 does not imply sources' modifications and may be hence immediately implemented.

5.2 Impact of power diversity

The second set of results, obtained adopting $i_{\max} = 10$, shows the throughput as a function of the input load for IDIC-1 in LOS (Fig. 4(a)) and NLOS (Fig. 4(b)) conditions, and for IDIC-2 in LOS and slow (Fig. 5(a)), NLOS and slow (Fig. 5(b)), LOS and fast (Fig. 5(c)), NLOS and fast (Fig. 5(d)) fading conditions. Notice that, for IDIC-2, it is worth to distinguish between slow and fast (mid- and small-scale) fading scenarios. More precisely, in a slow fading scenario, the two copies of a packet are subject to the same shadowing and fading effects, obtained by using the same realizations of the corresponding r.v.s. In a fast fading scenario, instead, the two copies are subject to two independent realizations of each of the respective r.v.s. Each of the six plots reports three curves, corresponding to the presence of
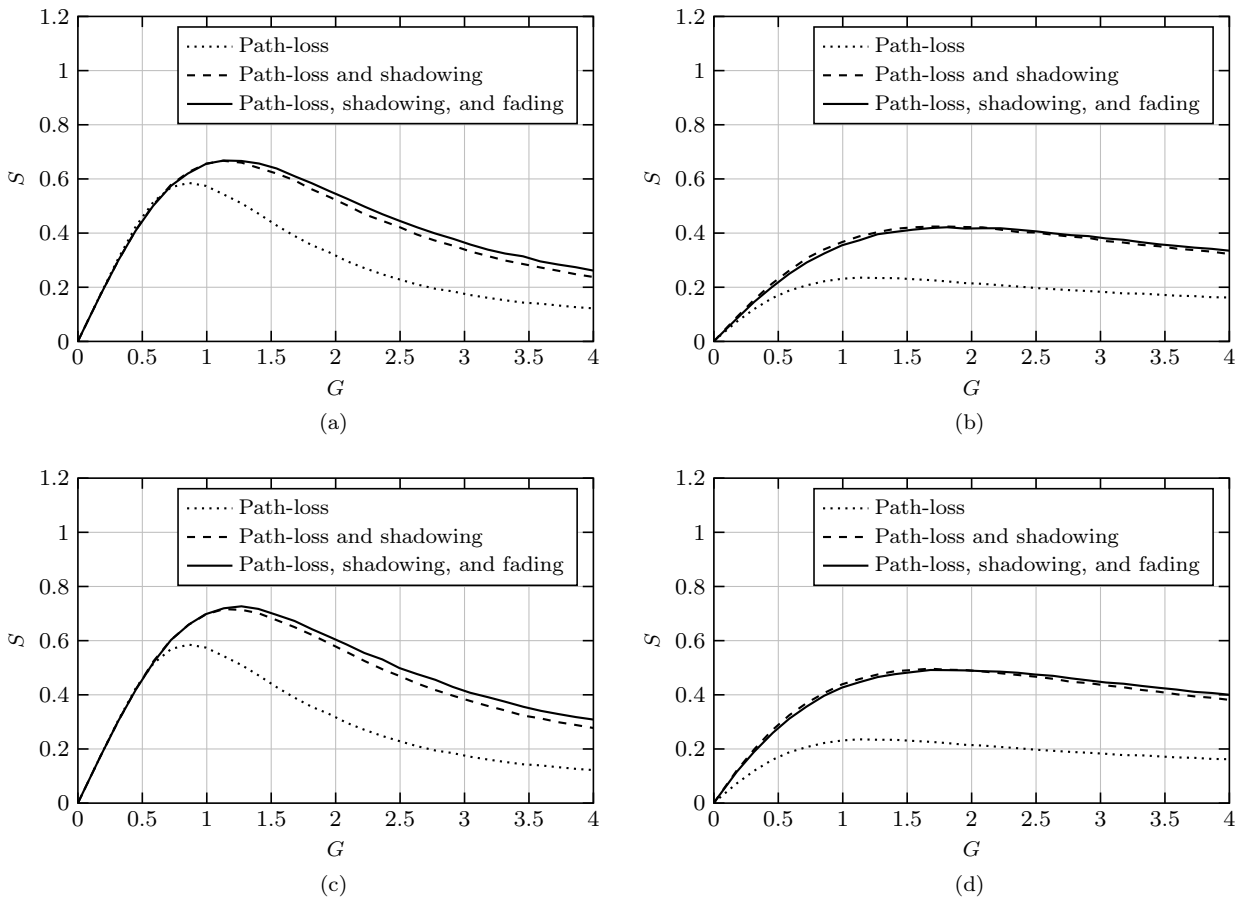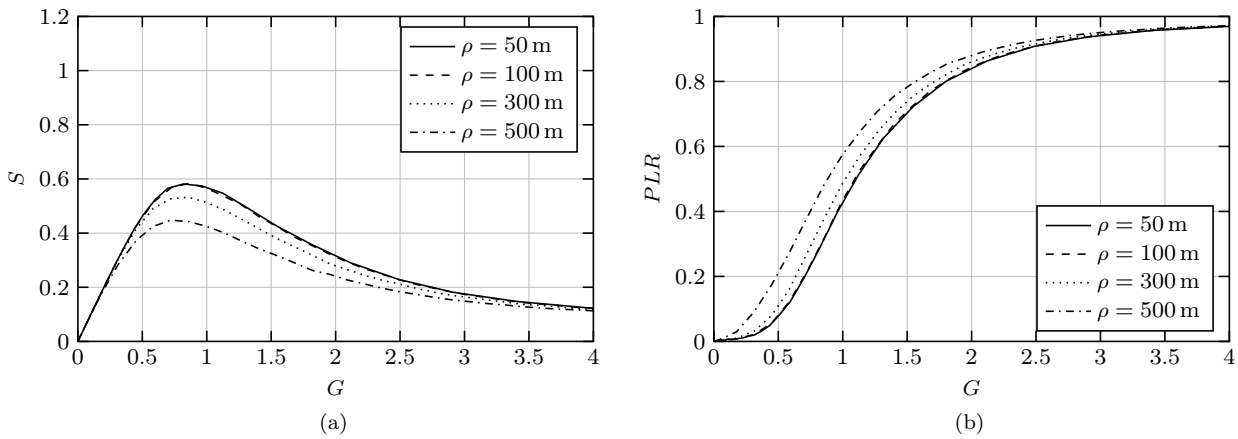
Fig. 5 Throughput vs. input load for IDIC-2 with $i_{\max} = 10$ in different channel conditions: (a) LOS and slow fading scenario, (b) NLOS and slow fading scenario, (c) LOS and fast fading scenario, (d) NLOS and fast fading scenario.

sole path-loss attenuations, the presence of both path-loss and shadowing, and, finally, the presence of path-loss, shadowing, and fading.

The first observation that can be formulated from this second set of figures concerns the benefits generally introduced by any added form of power diversity. This result is also consistent with several studies developed for the conventional μWave channel. In the here investigated mmWave context, the presence of shadowing considerably increases the throughput with respect to the case of sole path-loss, while the additional presence of small-scale fading usually provides a further slight improvement. Hence, the IDIC scheme properly operates in the propagation context that characterizes the mmWave environment, since it is not damaged by the substantially unavoidable mid- and small-scale fading effects, but, according to the NOMA concept, constructively exploits them as further sources of power diversity. Notice that, in the IDIC-2 cases, this consideration holds also when slow and fast fading scenarios are compared, since the second one, being characterized by the generation of independent shadowing and fading for

the two packet copies, introduces an additional power diversity effect among them that is not present in the slow fading scenario.

Concerning the adoption of packet diversity in a mmWave propagation environment, the optimality of the hybrid approach, consisting in the usage of IDIC-2 for low G values and of IDIC-1 for the higher G ones, is confirmed by the provided results. Interestingly, except for very high channel loads, the LOS scenario results always preferable than the NLOS one. This, intuitively, might seem an expected behavior, but, on a closer inspection, suggests a deeper consideration. Since all the investigated LOS (NLOS) scenarios are homogeneous, in the sense that all users (SoI and interferers) experience the same LOS (NLOS) conditions, the higher throughput in the LOS cases reveals that having a SoI directly visible is preferable to having all the interferers partially obstructed. This behavior confirms one of the most relevant differences between the mmWave and the so far realized μWave communications [33], in which the reduction of the interference has represented the main concern [28].

Fig. 6 Throughput (a) and PLR (b) vs. input load for different values of the cell radius in LOS conditions using IDIC-2 with $i_{\max} = 10$.
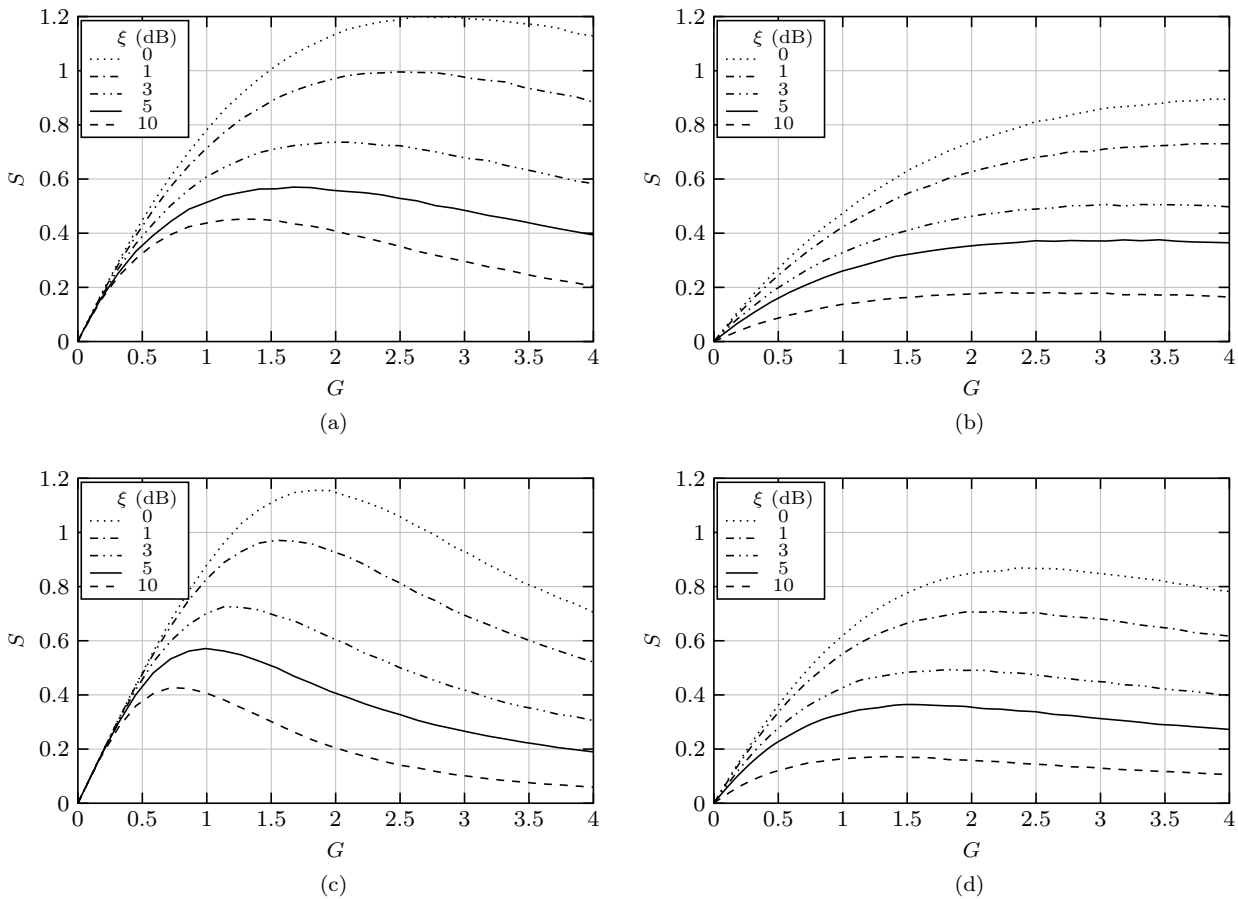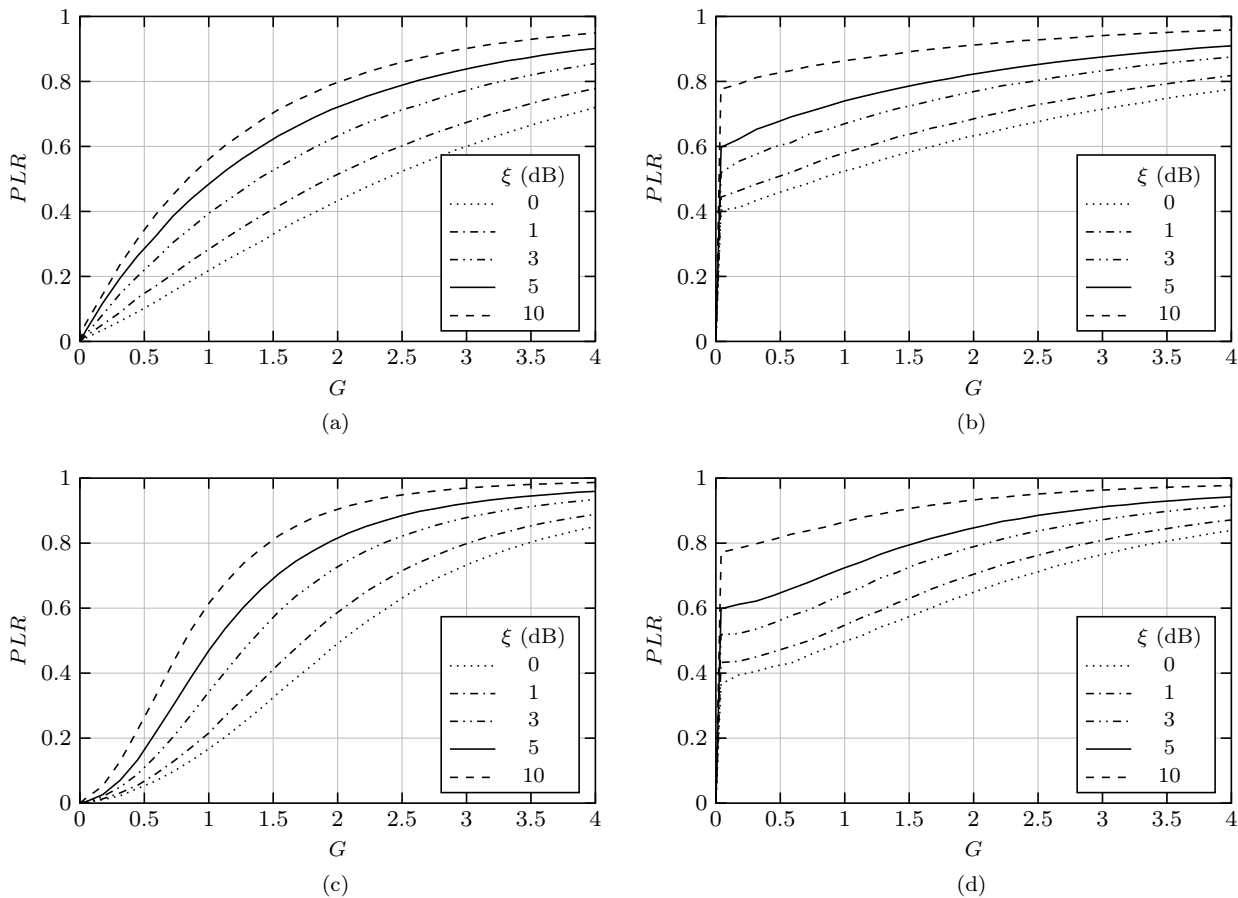

Fig. 7 Throughput vs. input load in the presence of path-loss, shadowing, and fading for $i_{\max} = 10$ and different SINR thresholds: (a) IDIC-1 in LOS conditions, (b) IDIC-1 in NLOS conditions, (c) IDIC-2 in LOS and fast fading conditions, (d) IDIC-2 in NLOS and fast fading conditions.

5.3 Impact of the cell radius

The third set of results explores the influence of the cell radius on the IDIC-2 performance. Fig. 6 reports the throughput (Fig. 6(a)) and the PLR (Fig. 6(b)) of

IDIC-2 as a function of the input load for different values of ρ in LOS conditions with $i_{\max} = 10$. As expected, an increase of ρ leads to a reduction of the throughput and an increase of the PLR. These degradations are however not so significant that making the receiving

Fig. 8 PLR vs. input load in the presence of path-loss, shadowing, and fading for $i_{\max} = 10$ and different SINR thresholds: (a) IDIC-1 in LOS conditions, (b) IDIC-1 in NLOS conditions, (c) IDIC-2 in LOS and fast fading conditions, (d) IDIC-2 in NLOS and fast fading conditions.

procedure ineffective. Rather, these results show that, even considering very large cells with respect to those commonly assumed for the mmWave context, IDIC-2 remains operative. In particular, maintaining the cell radius within the typically assumed value $\rho = 100$ m, the performance degradation is negligible. Furthermore, recent measurements reveal that cell radii larger than 200 m should not be adopted [3]. Under this requirement, the IDIC-2 performance experiences a really limited reduction. This puts into evidence a certain robustness of IDIC with respect to the specific deployment of the 5G base stations.

5.4 Impact of the SINR threshold

The final set of results, still obtained adopting $i_{\max} = 10$, shows the impact of the SINR threshold on the throughput for IDIC-1 in LOS (Fig. 7(a)) and NLOS (Fig. 7(b)) conditions, and for IDIC-2 in LOS and fast (Fig. 7(c)), and NLOS and fast (Fig. 7(d)) fading conditions. Each plot considers five SINR thresholds $\xi \in$

$\{0, 1, 3, 5, 10\}$ (dB) and is derived including path-loss, shadowing, and fading.

These results confirm that the adoption of a lower SINR threshold provides a higher throughput, thanks to the increase of the capture probability due to the relaxation of the reception requirement. However, since the threshold is also related to the modulation and the coding rate of the channel encoder implemented at the PHY layer, it cannot be inferred that a higher throughput efficiency directly implies a higher aggregate data rate. What instead may be reliably predicted is that, adopting a lower ξ value, a higher number of communications will become sustainable. Therefore, if the objective is to improve the fairness within the 5G cell, the usage of a low threshold may help to guarantee the connectivity to more users. The importance of the parameter ξ in the mmWave context may be emphasized recalling the space limitations reserved to the antenna system on a user's device. These limitations may be assumed similar to those on a μWave device in terms of absolute dimensions, but, being the single mmWave radiating

element much smaller, many antennas can be deployed on a 5G device in agreement with the massive MIMO paradigm. However, typically, no more than $K = 32$ elements are considered deployable on a Ka- or V-band transceiver [3]. This limits the maximum transmitting antenna power gain that can be reached to compensate the mmWave channel attenuations. To maintain an acceptable coverage within the 5G cell when these attenuations become consistent and cannot be compensated by the gains of the transmitting/receiving antennas, the basic element on which the system designer can still act is the SINR threshold ξ, namely, in practice, the code-modulation pair. This latter issue is more clearly put into evidence by Fig. 8, which reports the PLR corresponding to the four cases considered in Fig. 7. One may in particular notice from this figure that, in NLOS conditions, the PLR becomes significant even for low channel loads, while for higher G values the interference remain the main responsible of the higher losses.

A final observation that may be formulated regarding this last set of results concerns the appearing of some differences in the maximum throughput and PLR between IDIC-1 and IDIC-2 for the lower ξ values. This might represent a possible reason for preferring IDIC-1, which presents the higher maximum S values and the lower PLR ones, thus resulting more versatile in exploiting the code-modulation pair adopted at the PHY layer. This motivation may be considered beside the other previously discussed one, regarding the simpler implementation of IDIC-1, which, similarly to conventional framed SA, does not require the introduction of packet diversity. However, in general, from the reported results referred to the mmWave domain, the preferable solution for the receiver of a 5G BS in an uplink contention-based context seems to remain an adaptive IDIC-L approach in which the number of packet copies L is selected according to the offered load G and the SINR threshold ξ.

6 Conclusions

In this work, we have introduced IDIC-L, a novel receiver operation model for uplink random access at 5G BSs. The receiver, which is based on iterative decoding and interference cancellation, is capable of exploiting power and packet diversity through radio capture. The IDIC-L performance, properly obtained considering imperfect cancellation and realistic mmWave channel conditions, has shown improvements when compared to the widely adopted CRDSA scheme with ideal and noideal SIC. Beside the improved throughput, the specific IDIC-1 receiver, which operates in the presence of a unique packet copy and results more versatile in adapting to

the physical layer components, yields the advantage of being backward compatible with legacy SIC-enabled framed SA systems. In fact, since both framed SA and IDIC-1 rely on one packet copy, no changes are needed at the transmitter side, while just interference cancellation capabilities, already assumed by CRDSA, are required at the receiver side.

The results have however put into evidence that, in general, the preferable strategy in terms of packet diversity is to adapt the number of transmitted packet copies to the channel load and to the adopted code-modulation-pair, thus implementing a hybrid IDIC-1 / IDIC-2 approach so as to maximize the throughput and reduce the PLR in each occurring scenario. From a conceptual point of view, the here proposed study suggests that the opportunity of sending multiple packet copies, as done by repetition-based schemes, may be tightly connected to the combined assumptions of perfect interference cancellation and equal receive power (i.e., no capture). An intuitive interpretation of this relation may be formulated in terms of distortion of the cost/benefit balance that is assumed when packet diversity is applied neglecting the SINR conditions. In fact, on one hand, the cost of the increased channel load due to the additional packet copies may be underestimated by the assumption of very low power residual after cancellation. On the other hand, the benefit of transmitting additional copies to increase the probability of successful decoding may result amplified by the absence of capture. When these assumptions are relaxed, the traditional strategy of sending a single packet copy per frame may become again preferable in some scenarios, depending on the traffic that must be sustained in the 5G cell and on the PHY layer capabilities of the mmWave communicating devices.

References

1. J.G. Andrews, S. Buzzi, W. Choi, S.V. Hanly, A. Lozano, A.C.K. Soong, and J.C. Zhang. What will 5G be? *IEEE J. Sel. Areas Commun.*, 32(6):1065–1082, Jun. 2014.
2. M. Di Renzo. Stochastic geometry modeling and analysis of multi-tier millimeter wave cellular networks. *IEEE Trans. Wireless Commun.*, 14(9):5038–5057, Sep. 2015.

3. M.R. Akdeniz, Y. Liu, M.K. Samimi, S. Sun, S. Rangan, T.S. Rappaport, and E. Erkip. Millimeter wave channel modeling and cellular capacity evaluation. *IEEE J. Sel. Areas Commun.*, 32(6):1164–1179, Jun. 2014.

4. M.K. Samimi, G.R. Mac Cartney Jr., S. Sun, and T.S. Rappaport. 28 GHz millimeter-wave ultrawideband small-scale fading models in wireless channels. In *IEEE Vehic. Technol. Conf.*, 2016.

5. F. Babich, M. Comisso, and A. Cuttin. Impact of interference spatial distribution on line-of-sight millimeter-wave communications. In *IEEE Europ. Wireless*, pages 1–6, May 2017.

6. Y. Yaman and P. Spasojevic. Reducing the LOS ray beamforming setup time for IEEE 802.11ad and IEEE 802.15.3c. In *IEEE Military Commun. Conf.*, 2016.

7. A. Benjebbour, K. Saito, A. Li, Y. Kishiyama, and T. Nakamura. Non-orthogonal multiple access (NOMA): Concept and design. In *Signal processing for 5G: Algorithms and implementations*, chapter 7, pages 143–168. John Wiley & Sons, Ltd Chichester, UK, 2016.

8. B. Błaszczyszyn and P. Mühlethaler. Interference and SINR coverage in spatial non-slotted Aloha networks. *Ann. Telecommun.*, 70(7):345–358, Aug 2015.

9. F. Babich, M. Comisso, A. Crismani, and A. Dorni. On the design of MAC protocols for multi-packet communication in IEEE 802.11 heterogeneous networks using adaptive antenna arrays. *IEEE Trans. Mobile Comput.*, 14(11):2332–2348, Nov. 2015.

10. D. Espes, X. Lagrange, and L. Suárez. A cross-layer MAC and routing protocol based on Slotted Aloha for wireless sensor networks. *Ann. Telecommun.*, 70(3-4):159–169, Apr. 2015.

11. H. Singh and S. Singh. Smart-Aloha for multi-hop wireless networks. *Mobile Netw. Appl.*, 10(5):651–662, Oct. 2005.

12. Y. Chen, Y. Shen, J. Zhu, X. Jiang, and H. Tokuda. On the throughput capacity study for Aloha mobile ad hoc networks. *IEEE Trans. Commun.*, 64(4):1646–1659, April 2016.

13. W. T. Toor, J. Seo, and H. Jin. Distributed transmission control in multichannel s-Aloha for ad-hoc networks. *IEEE Commun. Lett.*, 21(9):2093–2096, Sep. 2017.

14. S. Sen, N. Santhapuri, R.R. Choudhury, and S. Nelakuditi. Successive interference cancellation: Carving out MAC layer opportunities. *IEEE Trans. Mobile Comput.*, 12(2):346–357, Feb. 2013.

15. E. Casini, R. De Gaudenzi, and O. del Rio Herrero. Contention resolution diversity slotted ALOHA (CRDSA): An enhanced random access scheme for satellite access packet networks. *IEEE Trans. Wireless Commun.*, 6(4):1408–1419, Apr. 2007.

16. DVB Document A155-2. *Digital Video Broadcasting (DVB); Second Generation DVB Interactive Satellite System (DVB-RCS2); Part 2: Lower Layers for Satellite standard*, 2017.

17. G. Liva. Graph-based analysis and optimization of contention resolution diversity slotted ALOHA. *IEEE Trans. Commun.*, 59(2):477–487, Feb. 2011.

18. E. Paolini, G. Liva, and M. Chiani. Coded slotted ALOHA: A graph-based method for uncoordinated multiple access. *IEEE Trans. Inf. Theory*, 61(12):6815–6832, Dec. 2015.

19. P. Tortelier and D. Le Ruyet. Erasure correction-based CSMA/CA. *Ann. Telecommun.*, 72(11-12):653–660, Dec. 2017.

20. H. Bui, K. Zidane, J. Lacan, and M. Boucheret. A multi-replica decoding technique for contention resolution diversity slotted Aloha. In *IEEE Vehic. Technol. Conf.*, pages 1–5, Sep. 2015.

21. N. Kuhn, O. Mehani, H.-C. Bui, E. Lochin, J. Lacan, J. Radzik, and R. Boreli. Improving web experience on DVB-RCS2 links. *Ann. Telecommun.*, 70(11-12):451–463, Dec. 2015.

22. A. Baiocchi and F. Ricciato. Analysis of pure and slotted Aloha with multi-packet reception and variable packet size. *IEEE Commun. Lett.*, 22(7):1482–1485, July 2018.

23. M. Chraiti, A. Ghrayeb, and C. Assi. A NOMA scheme for a two-user MISO downlink channel with unknown CSIT. *IEEE Trans. Wireless Commun.*, 17(10):6775–6789, 2018.

24. O. del Río Herrero and R. De Gaudenzi. Generalized analytical framework for the performance assessment of slotted random access protocols. *IEEE Trans. Wireless Commun.*, 13(2):809–821, Feb. 2014.

25. L. Vangelista, A. Zanella, and M. Zorzi. Long-range IoT technologies: The dawn of LoRa. In V. Atanasovski and A. Leon-Garcia, editor, *Future access enablers for ubiquitous and intelligent infrastructures*. Springer Int. Publishing, 2015.

26. F. Babich and M. Comisso. Including the angular domain in the analysis of finite multi-packet peer-to-peer networks with uniformly distributed sources. *IEEE Trans. Commun.*, 64(6):2494–2510, Jun. 2016.

27. H. Inaltekin, M. Chiang, H.V. Poor, and S.B. Wicker. On unbounded path-loss models: Effects of singularity on wireless network performance. *IEEE J. Sel. Areas Commun.*, 27(7):1078–1092, Sep. 2009.

28. G.L. Stuber. *Principles of mobile communication*. Norwell MA, Kluwer Academic Publishers, 1996.

29. A. Zanella and M. Zorzi. Theoretical analysis of the capture probability in wireless systems with multiple packet reception capabilities. *IEEE Trans. Commun.*, 60(4):1058–1071, Apr. 2012.

30. J.M. Holtzman. A simple, accurate method to calculate spread-spectrum multiple-access error probabilities. *IEEE Trans. Commun.*, 40(3):461–464, Mar. 1992.

31. F. Ricciato and P. Castiglione. Pseudo-random ALOHA for enhanced collision-recovery in RFID. *IEEE Commun. Lett.*, 17(3):608–611, Mar. 2013.

32. SAGE Millimeter Inc. Model SAO-2734030810-28-S1: Full Ka-Band Omnidirectional Antenna, 360 Degree, 7.5 dBi Gain, 2017.

33. S. Singh, R. Mudumbai, and U. Madhow. Interference analysis for highly directional 60-GHz mesh networks: The case for rethinking medium access control. *IEEE/ACM Trans. Netw.*, 19(5):1513–1527, Oct. 2011.

Response to reviewers' comments on:

Exploiting Capture and Interference Cancellation for Uplink Random Multiple Access in 5G Millimeter-Wave Networks

F. Babich[†], M. Comisso[†], A. Cuttin[†], F. Ricciato[§]

[†]Dept. of Engineering and Architecture (DIA), Univ. of Trieste (Italy)

[§]Faculty of Computer and Information Science, Univ. of Ljubljana (Slovenia)

I. RESPONSE TO THE EDITOR AND TO ALL REVIEWERS FOR PAPER ANTE-D-18-00173

We wish to thank the Editor for managing the review process and all of the referees for their constructive comments, which have prompted us to improve the submitted manuscript. According to these comments, we have inserted, in the revised paper, a theoretical analysis of the capture probability at the first iteration. Besides, we have added more details on the adopted parameters, more explanations on the considered performance figures and on the derived mathematical equations, finally providing a more extended and recent literature overview. A careful review of the text has been also carried out. To simplify the identification of the main introduced modifications, the text added to the revised paper has been written in red color. We did our best to address all the observations, providing a revised version of the paper that includes a detailed response to the reviewers' comments.

II. REVIEW PAPER ANTE-D-18-00173 NO1

The authors present an Iterative Decoding and Interference Cancellation method for 5G networks. The problem well defined and related to the state of the art. The authors consider the presence of cancellation residuals and capture, and propose a relatively realistic solution. The solution proposed by the authors sounds and has good potential as shown by the simulation results.

We would like to thank the referee for reviewing the presented manuscript and for the provided positive judgment. In agreement with the formulated observations, the paper has been carefully revised to clarify the outlined issues. Here is our detailed response to the reviewer's comments.

There are some minor issues to be checked before publishing the paper:

1) *How the value of the fraction of residual interference and the maximum number of SIC iterations are chosen.*

   The value γ for the fraction of the residual interference has been selected according to [29], where, among the possibilities investigated in that study, $\gamma = 0.1$ has been identified as a good compromise between an overly optimistic situation ($\gamma = 0$) and a scenario where the presence of the residual makes the SIC process ineffective ($\gamma = 0.5$). In the novel version of the paper, this comment has been reported in the second paragraph of Section 4.

   The value $i_{\max}$ for the maximum number of SIC iterations has been chosen to highlight the characteristics of the IDIC receiver in the different scenarios, while considering $i_{\max} = 10$ as a limit to avoid the running of too many iterations. One, of course, can let the IDIC receiver to evolve until all the resolvable collisions are identified, thus not imposing an $i_{\max}$ limit. However, this possibility presents significant practical drawbacks, since the improvement gained by the iterative algorithm decreases as $i_{\max}$ increases, and, simultaneously, both the processing delay and the computational burden increase. In other words, the efficiency of the SIC process decreases for $i_{\max}$ values larger than those adopted in the manuscript, while $i_{\max} = 10$ provides a satisfactory compromise between throughput gain and computational requirements. In the novel version of the paper, these observations have been summarized in the first paragraph of Subsection 5.1.

2) *As there is no mathematical model for the performance of the method. The authors should provide more simulation results with different values of the used parameters.*

To address this issue, in the revised manuscript we have developed a theoretical analysis for the estimation of the capture probability at the first iteration (i.e., for $i = 1$). The choice of modeling the capture event at the sole first iteration is motivated by the complexity required to calculate the capture probability for the subsequent iterations. In fact, for $i \geq 2$, the power of the packets captured at the previous iterations is partially or completely removed (depending on the γ value), thus the set of realizations of the remaining random variables corresponds just to the most degraded packets. The modeling of this set, which should account for the correlation among the remaining interference at the different iterations, is a rather difficult task, which, to the best of authors' knowledge, has not been even addressed in the literature. The developed analysis for $i = 1$ has been inserted in the novel Section 3 (Capture analysis), and the corresponding validation, i.e., the comparison between theoretical values and simulations, has been presented in the novel Subsection 3.1 (Validation) and in the novel Fig. 1.

Beside the capture analysis, Fig. 6 and Subsection 5.3 have been added to the revised paper, with the aim of illustrating the performance obtained by IDIC-2 for different values of the cell radius ρ. Is it worth noting that this parameter has required an increase until values $\rho > 100\,\text{m}$ to observe a noticeable throughput variation. This means that the IDIC algorithm maintains a stable performance throughout the range of values typical for a 5G cell radius. This exploration can be considered together with those concerning the maximum number of iterations i_{max} and the SINR threshold ξ to obtain an exhaustive insight on the performance behavior of the IDIC algorithm with respect to the physical parameters.

3) *Compare to the results to the method in [26].*

For the reply to this comment, we refer to the numbering of the references adopted in the revised paper, where the old item [26] corresponds to the new item [31]. The work in [31] enables the receiver to identify the slot positions where the same packet was transmitted in

all the past RAFs, and therefore cancel it from the signals received in further RAFs. Beside certain system-level details that are central to that work (e.g., pseudo-random slot selection based on payload content), the method in [31] corresponds to the extension of the IDIC-1 scheme towards inter-frame cancellation. Consequently, under an identical load scenario, the IDIC-1 throughput (with only intra-frame cancellation) represents a lower bound for the throughput achievable by [31]. Comparing intra- and inter-frame cancellation techniques involves the exploration of the inherent trade-off between throughput and computational resources (mainly memory, to store I/Q samples from past frames), plus a number of other system-level aspects. For these reasons, in the present contribution, we focus exclusively on intra-frame cancellation, leaving the analysis of the inter-frame extension in the mmWave context to future separate studies, which are included among the objectives of our ongoing activity. In summary, when referred to the sole intra-frame cancellation, the here presented scheme, represents an extension of [31] for what concerns its application to the mmWave channel and the possibility of transmitting L copies of a packet in a RAF (in [31], the transmission of just one copy per RAF is assumed). Instead, when referred to inter-frame cancellation, [31] is an extension of the sole IDIC-1 scheme (i.e., for $L = 1$), validated in a Rician fading channel. To clarify these aspects in the revised paper, the above considerations have been summarized in the third paragraph of Section 4.

4) *Some English corrections are needed, e.g. "the ideal estimation of the received signal amplitude, of the carrier frequency offset, and of the packet timing, Unfortunately, estimation . . . ".*

The signaled typing error has been corrected replacing the comma after 'timing' by a full stop. Besides, according to the referee's advice, in the second version of the paper we have revised in detail the English language.

III. Review paper ANTE-D-18-00173 No2

The authors propose a frame slotted aloha based receiver operation model called IDIC for mmWave 5G systems. The idea of the proposed work seems sound and novelty of the work is up to date. The paper is generally well written, however, it lacks the mathematical formulation of the IDIC receiver parameters, which are evaluated in numerical results section.

We would like to thank the referee for reviewing the proposed study and for appreciating the presented results. Taking into account the provided constructive suggestions, we have carefully revised the paper. Here is our detailed response to the issues underlined by the reviewer.

Apart from this, following points must be considered.

1) *Instead of directly starting your proposed scheme in abstract it is suggested to write first 2-3 introductory sentences about the area of the work e.g., about the mmWave based 5G and receiver architectures in it.*

   According to the referee's request, in the novel version of the paper the Abstract has been modified, so as to provide a brief introduction of the 5G mmWave context before the description of the proposed IDIC receiver.

2) *Equation (1) explanation is not clear. Especially, the information about the PDF and its derivation from (2). Please, describe what is ρ in (2)?*

   In the revised manuscript, we have better explained the physical meaning of the quantities in (1). Besides, we have reported, in the novel equation (2), the probability density function of a uniform distribution over a disk $\mathrm{D}(O, \rho)$ in polar coordinates, where ρ represents the radius of the 5G cell. By integrating (1) on the angle in the domain $[0, 2\pi[$ and then integrating on the distance d_m, one finally obtains the cumulative distribution function in (3), which will be used in the added Section 3 for the capture analysis.

3) *Apart from the algorithm given in Section 3, reviewer cannot find any mathematical description of the performance evaluation parameters related to IDIC receivers.*

In order to clarify this aspect, the mathematical expressions for the throughput S and for the packet loss ratio PLR have been added to the revised paper. In particular, S is evaluated by randomly generating $V = 100$ user topologies within the disk, and subsequently simulating $H = 1000$ RAFs for each topology. By consequence, the throughput is estimated by averaging the results over the topologies and the RAFs according to:

$$S = \frac{1}{V} \sum_{v=1}^{V} \left[\frac{1}{H} \sum_{h=1}^{H} \frac{\mathcal{A}_{h,v}^{i_{\max}}(G)}{N} \right],$$ (1)

where $\mathcal{A}_{h,v}^{i_{\max}}(G)$ is the number of packets successfully decoded in the h-th RAF and v-th topology after $i_{\max}$ iterations for an input load G, while N is the number of time slots contained in a single RAF. The PLR is then calculated from S as:

$$PLR = 1 - \frac{S}{G}.$$ (2)

These specifications have been inserted in the first paragraph of Section 5.

4) *The performance parameters evaluation lacks the analytical analysis. Only Monte-Carlo simulations are performed, which raises concerns about the soundness of the proposed work.*

To address this issue, in the second version of the paper we have added the capture analysis at the first iteration. This analysis, developed in Section 3 (Capture analysis) provides a theoretical estimation of the capture probability considering path-loss attenuation, shadowing, small-scale fading, interference, and noise. The analysis is validated in Subsection 3.1 (Validation) and in the novel Fig. 1, which shows a significant agreement between the theoretical values (represented by lines) and the corresponding simulations (represented by markers).

5) *Please rephrase the following sentences for clarity. It is also generally suggested that instead of writing in longer sentences, use simple and short sentences.*

   a. *This capability makes interesting a comparison, in the mmWave context, with the widely adopted CRDSA scheme, which is characterized by the usage of $L = 2$ replicas of each packet in the RAF [13].*

b. *The PLR, which is still reported as a function of G, represents instead the fraction of successfully received packets with respect to the transmitted ones, and accounts for the losses due to both the propagation environment and the interference.*

c. *However, **mmWAve** 5G systems are affected by several propagation phenomena, such as small- and mid-scale fading, which may have a strong impact on the final result of a communication. Correct the bold word.*

In the novel version of the manuscript, the identified sentences (a) and (b) have been rephrased by splitting them in more parts to improve the readability, while the error signaled in (c) has been corrected.

6) *Although the authors have discussed about the capture effect, which is an important aspect of this paper, in Introduction, it is suggested to explain its basics in one or two sentences.*

According to the referee's request, in the revised paper we have added two introductory sentences on the capture effect in the third paragraph of Section 1.

7) *Majority of references are not from the recent years. It is suggested that more than 50% of references should be from the last two to three years.*

Following the reviewer's suggestion, in the second version of the paper we have revised the bibliography by replacing, when possible, the previous references with more recent ones. In the currently submitted manuscript, 60% of the cited works has been published in the range between 2015 and 2018.

IV. REVIEW PAPER ANTE-D-18-00173 No3

A new receiver is proposed for uplink mmWave cellular networks. The receiver design exploits the process of decoding and IC to resolve collisions within each frame. The authors proposed a propagation model leveraging some new measurements for the mmWave channel. Numerical results are presented to study the performance by studying the performance (throughput vs. load) as a function of power. The mmWave technology is a new 5G technology that offers much higher bandwidth and therefore promises to achieve higher rates. This paper makes a good contribution in the uplink access. The receiver design seems to be performing well. The paper is also generally well written and hence can be recommended for publication after some minor changes.

We would like to thank the referee for reviewing the submitted paper as well as for the positive evaluation of the conceived work. The recommended adjustments and explanations have been introduced in the revised manuscript. Here is our response to each specific reviewer's comment.

1) *I would like the author to give more details of their simulation environment. Did they only numerical evaluate their receive design by solving the models derived or they did some monte carlo simulation for their evaluation? I did not see comparison between simulations and numerical evaluation.*

   In the previous version of the manuscript, only simulation results were presented. Instead, in the revised paper, we have inserted the theoretical estimation of the capture probability at iteration $i = 1$ in the novel Section 3 (Capture analysis). This analysis accounts for path-loss attenuation, shadowing, small-scale fading, interference, and noise, and describes a mathematical model to approximate the probability of capturing a packet in a slot. The analysis is validated in Subsection 3.1 (Validation) and in the novel Fig. 1. This figure reports the theoretical values (represented by lines) and the corresponding simulations (represented by markers), revealing a significant agreement between the two approaches that confirms the accuracy of the formulated theoretical estimation. The performance figures shown in Figs. 2-8 are all obtained by Monte Carlo simulations, because of the significant complexity in theoretically modeling the throughput for an iterative SIC system in the

presence of capture, which, to the best of the authors' knowledge, still remains an open issue not even addressed in the literature.

2) *There is a new technique that performs much better than interference cancellation, which is called interference dissolution: M. Chraiti, et.al.: Interference Management in a One-dimensional Space: Interference Dissolution. CoRR abs/1606.06021 (2016). Can the authors also elaborate whether this method can be of value for their design?*

We thank the referee for the signaled work, which has been added to the bibliography of the revised paper as reference [23]. The Interference Dissolution (ID) approach presented in [23] requires modifications both at the transmitter and receiver sides, while our aim is to consider a decoding method that: (i) can be implemented exclusively on the receiver side, without requiring changes on the transmitter; and (ii) is insensitive to the specific modulation scheme, thus being directly applicable also to legacy wireless devices. The sequential cancellation scheme proposed in our work is studied to meet these requirements, making it suitable for already deployed systems. Of course, by removing such requirements (design constraints) and allowing for a "clean slate" design of the modulation format and of the transmitter operation, one can achieve a higher throughput performance at the cost of a reduced backward compatibility with respect to legacy systems. In other words, like other system designs and engineering problems, a trade-off is in place between generality and ease of adoption on one hand, and performance on the other. The method considered in our work and the ID approach in [23] hence lie at the opposite ends of this trade-off, where our method is more focused on compatibility, while [23] is more oriented towards performance. In the revised paper, this discussion has been summarized at the end of the second paragraph of the Introduction.